[논 문] 한국재료학회지
Korean J. Mater. Res.
Vol. 31, No. 7 (2021) https://doi.org/10.3740/MRSK.2021.31.7.382

Linear and Nonlinear Optical Properties of Vanadium Pentoxide Films Prepared by Pulsed-Laser Deposition

Liqi Cui, Ruiteng Wang, and Weitian Wang†

Institute of Opto-Electronic Information Science and Technology, Yantai University, Yantai 264005, P.R. China

(Received January 15, 2021 : Revised June 21, 2021 : Accepted June 21, 2021)

Abstract Well-crystallized vanadium pentoxide V_2O_5 thin films are fabricated on MgO single crystal substrates by using pulsed-laser deposition technique. The linear optical transmission spectra are measured and found to be in a wavelength range from 300 to 800 nm; the data are used to determine the linear refractive index of the V_2O_5 films. The value of linear refractive index decreases with increasing wavelength, and the relationship can be well explained by Wemple's theory. The third-order nonlinear optical properties of the films are determined by a single beam *z*-scan method at a wavelength of 532 nm. The results show that the prepared V_2O_5 films exhibit a fast third-order nonlinear optical response with nonlinear absorption coefficient and nonlinear refractive index of 2.13×10^{-10} m/W and 2.07×10^{-15} cm^2/kW, respectively. The real and imaginary parts of the nonlinear susceptibility are determined to be 3.03×10^{-11} esu and 1.12×10^{-11} esu, respectively. The enhancement of the nonlinear optical properties is discussed.

Key words nonlinear, optical properties, transition metal oxides, pulsed-laser deposition.

1. Introduction

Linear and nonlinear optical materials with higher order nonlinearity have great potentials in the field of opto-electronics. It has been shown that the large third-order nonlinear optical coefficient $c^{(3)}$ and fast response time are important for promising applications in nonlinear optical devices such as saturable absorbers and optical limiters.[1-4] Many studies show that host dielectric materials containing nanometer-sized metal or semiconducting particles exhibit enhanced $c^{(3)}$ as a result of the localized surface plasmon resonances due to the presence of confined electrons.[5,6] The observed $c^{(3)}$ is highly sensitive to size and shape of the nanoparticles. However, there are some restrictions for these composite materials in practical applications because of the existing large linear resonant absorption.

Transition metal oxide films with good transparency are considered to be promising nonlinear optical materials which can be ascribed to their high refractive indices and localized electrons on the basis of Miller's rule.[7,8] The third-order nonlinear optical responses of TiO_2, Nb_2O_5, Ta_2O_5 were reported.[9,10] According to the bond-orbital theory,[11] the *d*-orbital contributions to nonlinear response are found to increase rapidly as a function of decreasing bond length *d*. The average bond length of vanadium pentoxide V_2O_5 (d = 1.83 Å) is shorter than that of TiO_2 (d = 1.96 Å), Nb_2O_5 (d = 2.00 Å), Ta_2O_5 (d = 2.04 Å). Compared with other transition metal oxides, the investigation of nonlinear optical properties of V_2O_5 is more attracting and meaningful.

In this paper, we report on the linear and third-order nonlinear optical properties of V_2O_5 films grown on MgO single crystal substrates by using pulsed-laser deposition technique. The linear optical transmission spectra were measured in the wavelength range from 300 to 800 nm. The linear optical indices of the prepared films were extracted from the transmission data by a numerical method. The third-order nonlinear optical coefficient $c^{(3)}$ was investigated by a single beam *z*-scan method.[12,13] The results show that the well-crystallized V_2O_5 films exhibit a fast third-order nonlinear optical response, which may be attractive for potential applications for optical processing, computing, and optical limiting.

†Corresponding author
E-Mail : whetwang@163.com (W. T. Wang, Yantai Univ.)

2. Experimental Details

The V_2O_5 thin films were deposited using a Lambda Physic KeF excimer laser (λ = 248 nm) focused onto a high-purity ceramic target, which was prepared from the analytic reagent grade V_2O_5 powder. The structure and composition of V_2O_5 target was examined and confirmed by powder x-ray diffraction (XRD) using a Rigaku diffractometer with Cu $K\alpha$ radiation at λ = 1.54 Å. The target was mounted on a rotating holder, 40 mm from the MgO single crystal substrates which were polished on both sides for optical measurements. The chamber was evacuated to high vacuum of 1×10^{-4} Pa, following by the deposition carried out under an oxygen pressure of 30 Pa.

The substrates were maintained at 400 °C during the deposition process. The thickness of the fabricated V_2O_5 films was measured to be about 220 nm by a surface profile measuring system (DEKTAK, USA). The film crystallinity was characterized by XRD in the angular range of $20^o \leq 2\theta \leq 44^o$. The linear optical transmission spectra were measured in the wavelength range of 300 to 800 nm by using a SpectraPro-500i spectrophotometer (Acton Research Corporation) at room temperature in air.

The third-order nonlinear optical properties of the prepared V_2O_5 films were measured by using the single beam *z*-scan method. A Q-switched laser (λ = 532 nm) with a pulse duration of 55 ps was employed as the light source in order to investigate the fast responses. The laser beam was focused on the sample with a 120 mm focal length lens leading to a measured beam waist of ω_0 = 30 μm and a pulse energy of I_0 = 5.0 μJ at the focal plane. When the transmittance, which passed through the sample, was measured through a closed aperture (CA) placed in the far field, the z-scan curve was mainly affected by the beam distortion induced by the nonlinear refraction n_2, which can be used to calculate Re$c^{(3)}$, while the measurements performed with a open aperture (OA) revealed the nonlinear absorption β, which can be used to calculate Im$c^{(3)}$. The n_2 and β are defined by $n = n_0 + n_2I$ and $\alpha = \alpha_0 + \beta I$, respectively, where the n_0 and α_0 are the linear refractive index and linear absorption coefficient. The details of the z-scan measurements were reported elsewhere.[14,15]

3. Results and Discussion

Fig. 1 shows the typical θ-2θ XRD pattern of the V_2O_5 films grown on MgO (100) substrates. Besides the strong diffraction peak from the substrate, only sharp (00*l*) and (*l*00) peaks for the V_2O_5 films is observed in the range of $20^o \sim 44^o$, indicating the good purity and crystallinity of the prepared films. As is known, vanadium has many valence states, and there are correspondingly many vanadium oxides.

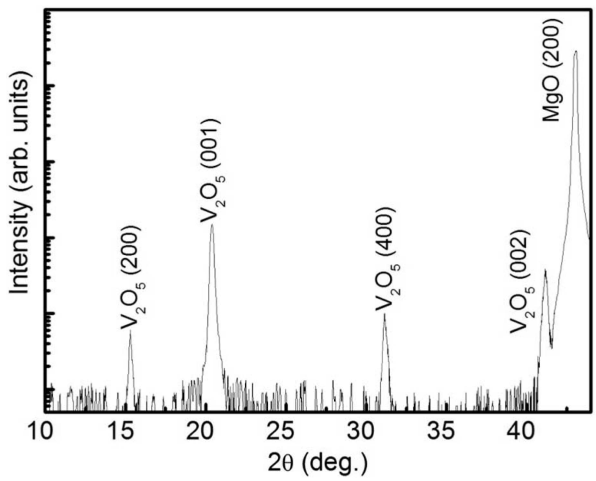

Fig. 1. Typical θ-2θ XRD pattern of V_2O_5 film on MgO (100) substrate.

The process for controlled growth and desired vanadium oxides needs careful adjustment of growth parameters and conditions. Among these oxides, V_2O_5 is the most stable compound. Moreover, the film was deposited under an oxygen pressure of 30 Pa to supply adequate oxygen for the fabrication of V_2O_5. Our result shows that stable single-phase V_2O_5 films can be fabricated on MgO substrates and no other oxide phases can be detected. By using the diffraction data, the lattice parameters a and c are determined as 11.58Å and 4.38 Å, respectively, which are in agreement with those in literature.[11)]

Fig. 2 shows the optical transmission spectra of the V_2O_5 films measured at room temperature. As for thin homogeneous films deposited onto transparent substrates, typical transmission spectra display oscillating curves that come from the interference effects. The envelopes represent simulated smooth lines passing through the extremes of the interference fringes. The upper and lower dashed lines, denoted respectively as T_M and T_m, can be used to calculate the linear refractive index n_0 which is given by[16)]

$$n_0^{\,2} = N + \left(N^2 - n_s^{\,2}\right)^{1/2}, \tag{1}$$

where

$$N = 2n_s \frac{T_M - T_m}{T_M T_m} + \frac{n_s^{\,2} + 1}{2}, \tag{2}$$

and n_s is the refractive index of the substrate. The determined n_0 of the V_2O_5 films is shown in Fig. 3. The value of n_0 decreases with increasing wavelength, suggesting the normal dispersion of V_2O_5 films in the range of 300 ~ 800 nm. According to Wemple's theory,[17)] the linear refractive index can be expressed as

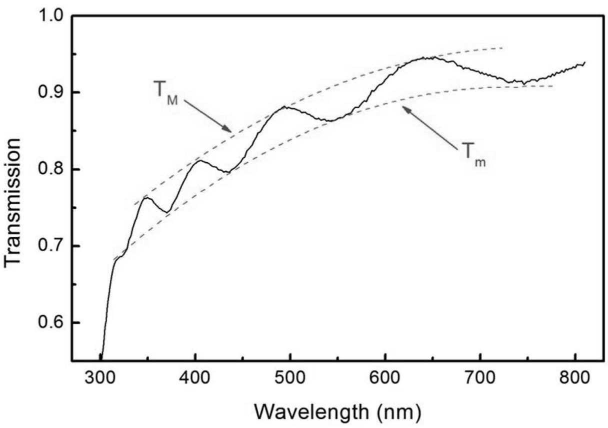

Fig. 2. Optical transmission spectrum for a prepared V_2O_5 film. The dashed lines indicate the simulated envelopes of the extremes of the interference fringes.

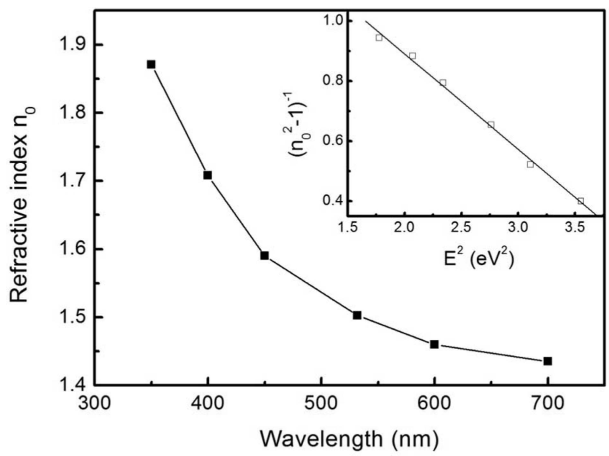

Fig. 3. The calculated refractive index for a V_2O_5 film as a function of wavelength. The inset shows the linear plots of $(n_0 - 1)$ versus E^2.

$$\frac{1}{{n_0}^2 - 1} = a - bE^2 , \tag{3}$$

where E is the photon energy in electron volt unit, a and b are constants related to the materials. The linear dependence of $1/(n_0 - 1)$ on E^2 is shown in the inset of Fig. 3.

A typical OA z-scan result for a V_2O_5 film is shown in Fig. 4 which corresponds to the far-field transmission as a function of its distance to the lens focus. The open circles denote the experimental transmittance, while the solid curve is the theoretical fit. At focus $z = 0$, the OA data comprise normalized transmittance peak, indicating the presence of nonlinear saturation. The theoretical fit is simulated by expression[18)]

$$T_{OA}(z) = \sum_{m=0}^{\infty} \frac{\left(-\beta I_0 L\right)^m}{\left(1 + z^2 / z_R^2\right)^m \left(1+m\right)^{3/2}} , \tag{4}$$

where L is the effective thickness of the film, and $z_R = \pi {\omega_0}^2 / \lambda$ is the Rayleigh length of the beam. The obtained β value was 2.13×10^{-10} m/W. The nonlinear absorption coefficient β is related to the imaginary part of the third-order nonlinear optical susceptibility Im$c^{(3)}$ by the following equation [19)]

$$\mathrm{Im}\, \chi^{(3)} = \frac{c^2 n_0^2}{240\pi^2 \omega} \beta , \tag{5}$$

where c is the speed of light in vacuum, ω is the angular frequency of the light field. The obtained Im$c^{(3)}$ was 1.12 $\times 10^{-11}$ esu.

Fig. 5 shows the CA z-scan result for a V_2O_5 film. The solid line is the theoretical fit. The CA curve exhibits peak-to-valley configuration, indicating the existence of nonlinear refractive index n_2. According to the theory described by Sheik-Bahae et al.,[12,13)] the presence of saturable absorption β enhances the peak and reduces the valley. Then the normalized CA transmittance, affected by n_2 in addition to β, is given by,[18)]

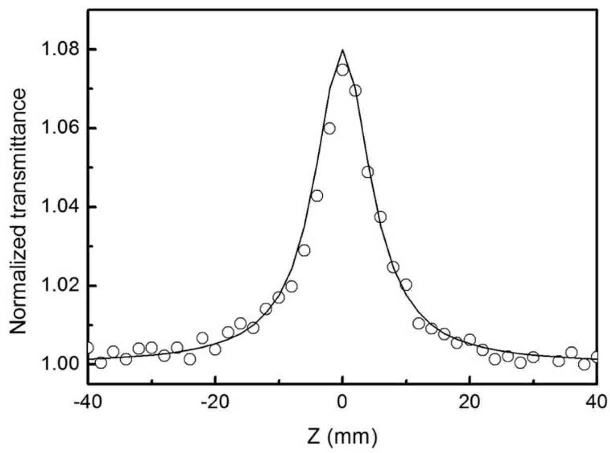

Fig. 4. OA z-scan result for a V_2O_5 film. The solid line indicates the theoretical fit.

$$T_{CA}(z) = 1 - \frac{\beta I_0 L \left(\frac{\gamma z^2}{z_R^2} + \frac{2z}{z_R} + 3\gamma \right)}{\gamma \left(\frac{z^2}{z_R^2} + 9 \right) \left(\frac{z^2}{z_R^2} + 1 \right)} , \tag{6}$$

where the factor

$$\gamma = \frac{c n_0 \lambda \beta}{160\pi^2 n_2} . \tag{7}$$

The calculated nonlinear refractive index n_2 of V_2O_3 film was 2.07×10^{-15} cm^2/kW. The nonlinear refractive index n_2 is related to the real part of the third-order nonlinear optical susceptibility Re$c^{(3)}$ by the following equation[19)]

$$\mathrm{Re}\, \chi^{(3)} = \frac{c n_0^2}{120\pi^2} n_2 . \tag{8}$$

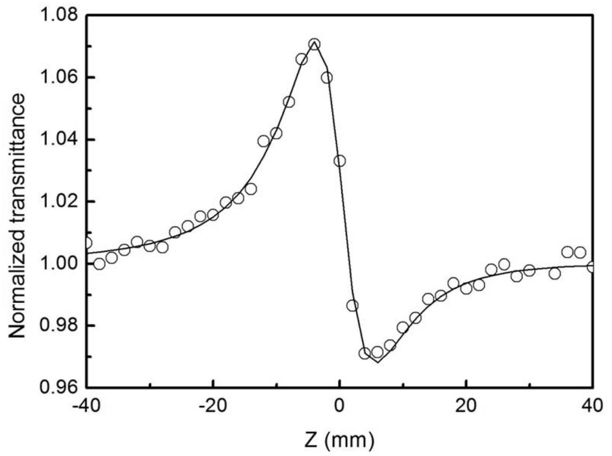

Fig. 5. CA *z*-scan result for a V_2O_5 film. The solid line indicates the theoretical fit.

The calculated $\mathrm{Re}c^{(3)}$ value was about 3.03×10^{-11} esu. It is worth noting that the obtained $c^{(3)}$ value of the prepared V_2O_5 films is $1 \sim 2$ orders larger than that of TiO_2, Fe_2O_3, Ta_2O_5 transition oxide films.[9,10] This is the result from the influence of the *d* orbitals on the linear and nonlinear optical properties based on the bond-orbital theory.[11] As the bond length of V_2O_5 is the shortest one, the nonlinear optical coefficient is larger than that of other transition oxides. Moreover, the fabricated V_2O_5 films were not single orientation because of the lattice mismatches between the films and substrates. Complex nanostructure and tower-like grains of V_2O_5 films were reported previously.[20] The nanostructure and morphology can improve the local fields near the grains and grain boundaries, which contribute much more to the enhancement of the nonlinear optical properties.

4. Conclusion

Well-crystallized V_2O_5 thin films were fabricated on MgO (100) substrates by using PLD technique. The linear and nonlinear optical properties have been investigated. The value of linear refractive index n_0 decreases with increasing wavelength, and the relationship can be well explained by Wemple's theory. A *z*-scan method was employed to measure the third-order nonlinear optical properties of the V_2O_5 films. The values of the real and imaginary parts of $c^{(3)}$ were determined to be 3.03×10^{-11} esu and 1.12×10^{-11} esu, respectively. The results suggest that transition metal oxide V_2O_5 films can be used in particular optical fields with special requirements.

Acknowledgement

The authors acknowledge the financial support from the National Natural Science Foundation of China under Grand No. 10704065.

References

1. H. Takacs, B. Viala, J. H. Tortai, V. Herman and F. Duclairoir, J. Appl. Phys., **119**, 093907 (2016).
2. S. Fraser, X. Zheng, L. Qiu, D. Li and B. Jia, Appl. Phys. Lett., **107**, 031112 (2015).
3. Y. S. Tamgadge, S. S. Talwatkar, A. L. Sunatkari, V. G. Pahurkar and G. G. Muley, Thin Solid Films, **595**, 48 (2015).
4. S. J. Lim, H. T. Kwak, D. Choi, S. Y. Park and N. Kim, Korean J. Mater. Res., **4**, 466 (1994).
5. S. Debrus, J. Lafait, M. May, N. Pincon, D. Prot, C. Sella and J. Venturini, J. Appl. Phys., **88**, 4469 (2000).
6. W. T. Wang, D. Y. Guan, G. Yang, G. Z. Yang, Y. L. Zhou, H. B. Lu and Z. H. Chen, Thin Solid Films, **471**, 86 (2005).
7. R. C. Miller, Appl. Phys. Lett., **5**, 17 (1964).
8. C. C. Wang, Phys. Rev. B, **2**, 2045 (1970).
9. T. Hashimoto, T. Yoko and S. Sakka, Bull. Chem. Soc. Jpn., **67**, 653 (1994).
10. T. Hashimoto, T. Yoko and S. Sakka, J. Ceram. Soc. Jpn., **101**, 64 (1993).
11. M. E. Lines, Phys. Rev. B, **43**, 11978 (1991).
12. M. Sheik-Bahae, A. A. Said, T. H. Wei, D. J. Hagan and E. W. V. Stryland, IEEE J. Quantum Electron., **26**, 760 (1990).
13. M. Sheik-Bahae, A. A. Said and E. W. V. Stryland, Opt. Lett., **14**, 955 (1989).
14. W. Wang, Y. Sun, Z. Dai and D. Guan, Acta Optica Sinica, **26**, 1 (2006).
15. W. Wang, C. Shi, X. Su, H. Xing and J. Zhang, Mater. Res. Bull., **41**, 2018 (2006).
16. R. Swanepoel, J. Phps. E: Sci. Instrum., **16**, 1214 (1983).
17. S. H. Wemple, J. Chem. Phys., **67**, 2151 (1977).
18. M. Yin, H. P. Li, S. H. Tang and W. Ji, Appl. Phys. B, **70**, 587 (2000).
19. P. B. Chapple, J. Staromlynska, J. A. Hermann and T. J. Mckay, J. Nonlinear Opt. Phys. Mater., **6**, 251 (1991).
20. Y. Deng, A. Pelton and R. A. Mayanovic, MRS Advances, **1**, 2737 (2016).

Author Information

Liqi Cui

Postgraduate Student, Institute of Opto-Electronic Information Science and Technology, Yantai University, China

Ruiteng Wang

Postgraduate Student, Institute of Opto-Electronic Information Science and Technology, Yantai University, China

Weitian Wang

Professor of Physics, Institute of Opto-Electronic Information Science and Technology, Yantai University, China.